Available online at www.sciencedirect.com
SCIENCE DIRECT®
Journal of the European Ceramic Society 26 (2006) 267–272
www.elsevier.com/locate/jeurceramsoc

Elaboration and mechanical characterization of nanocomposites thin films Part II. Correlation between structure and mechanical properties of SiO_2-PMMA hybrid materials

Fayna Mammeri[a,b], Laurence Rozes[a], Eric Le Bourhis[b], Clément Sanchez[a,*]

[a] *Université Pierre et Marie Curie, Laboratoire de Chimie de la Matière Condensée, UMR 7574 CNRS, Case 174, 4 Place Jussieu, 75252 Paris Cedex 05, France*
[b] *Université de Poitiers, Laboratoire de Métallurgie Physique, UMR 6630 CNRS, SP2MI-Téléport 2-Bd Marie et Pierre Curie, B.P. 30179, 86962 Futuroscope-Chasseneuil Cedex, France*

Received 25 July 2004; received in revised form 10 November 2004; accepted 21 November 2004
Available online 25 January 2005

Abstract

Mechanical properties of hybrid thin films based on SiO_2-PMMA materials were investigated through nanoindentation tests. We demonstrated in the part I of this paper, that nanoindentation is an appropriate technique to characterize hybrid organic–inorganic thin films. Specific procedures of analysis and the use of appropriate models allows to determine reproductive indentation modulus and hardness of the hybrid layers. The mechanical responses of nanocomposites are not only governed by the composition of the layers but also by the nature and the extent of the hybrid interface. Different layers have been studied, constituted by an inorganic and an organic phase that just be physically mixed or covalently connected. The weak (H bonds) or strong (covalent bonds) interactions generated by the hybrid interface lead to nanocomposites which exhibit different mechanical behaviours. Moreover, comparison between layers obtained by in situ inorganic polymerization in PMMA and layers obtained with preformed silica nano-particles have been also investigated to correlate the morphology of the nanocomposites with the mechanical responses.

Keywords: Nanocomposites; Mechanical properties; Sol–gel processes; Films; Nanoindentation; SiO_2; PMMA

1. Introduction

Mild synthetic conditions provided by sol–gel chemistry[1,2] (synthesis of glasses and ceramics from molecular precursors, such as metal alkoxides, by hydrolyse and condensation reactions in an organic solvent at room temperature) allows to incorporate organic components into an inorganic network, leading to hybrid organic–inorganic materials.[1,3–17] The degree of interpenetration of organic and inorganic components is ranged between the sub-micro and the nano scale level. Consequently, sol–gel routes provide an easy method to synthesize hybrid nanocomposites. Larger hybrid interfaces can be developed in nanocomposites than in classical composites (matrix reinforced by fibers for example) allowing to classify them according to their interfacial properties. The hybrid networks can be conveniently divided into two classes.[13] Class I corresponds to hybrid systems in which the two components exchange only weak interactions like hydrogen bonding whereas the organic and inorganic components are linked through covalent chemical bonds in class II materials.

Sol–gel chemistry offers a versatile route to design chemically a great variety of hybrid organic–inorganic materials.

* Corresponding author. Tel.: +33 1 44 27 55 34; fax: +33 1 44 27 47 69.
E-mail address: clems@ccr.jussieu.fr (C. Sanchez).

0955-2219/$ – see front matter © 2004 Published by Elsevier Ltd.
doi:10.1016/j.jeurceramsoc.2004.11.014

For example, can be mentioned the "simultaneous" formation of two networks from molecular precursors bearing both organic and inorganic functionalities,[9] the in situ polymerisation of metal alkoxides in preformed polymers,[18,19] the impregnation of porous inorganic networks by a solution of an organic monomer (followed by organic polymerisation),[20,21] the use of nanobuilding blocks or preformed nanoparticles[15,16,22] contributing to the flexibility of both the nature and the size of the hybrid interface.

In the part I paper, we reported the study of the mechanical properties of class II hybrid organic–inorganic thin films, prepared by the cocodensation of a triethoxysilane functionalized poly(methyl methacrylate) (f-PMMA) and a prehydrolyzed (in acidic conditions) solution of tetraethoxysilane (TEOS). We showed that instrumented nanoindentation allowed to determine the mechanical properties (indentation modulus and hardness) of the PMMA-SiO_2 hybrid thin films, which were strongly dependent on the organic–inorganic ratio.

In this present work, an investigation of the effects of the hybrid interface between the organic and inorganic components on the mechanical properties of PMMA-SiO_2 based hybrid thin films has been performed. Two main ways were chosen to modify the nature and the size of the hybrid interface. Firstly, class I hybrid materials were synthesized by the in situ polymerisation of TEOS in a free triethoxysilane groups PMMA;[23] in this case, and contrary to functionalized based hybrid materials (part I), the formation of covalent chemical bonds between the silica and the polymer is avoided. Secondly, class II hybrid materials were synthesized by introducing preformed and well calibrated silica nanoparticles (Ø 12 nm) in a triethoxysilane functionalized PMMA. Their mechanical properties were compared to the class II PMMA-TEOS hybrids reported in paper I.

2. Experimental procedures

2.1. Films preparation

2.1.1. Materials

Tetraethoxysilane (TEOS 99%) and [3-(methacryloxy)propyl]triethoxysilane (MPTES) were purchased from ABCR-Gelest, azobisisobutyronitrile (AIBN) from Fluka. The monomer methyl methacrylate (MMA 99% from Aldrich) was purified by distillation before use. Acetonitrile was dried over molecular sieve. The free triethoxysilane groups PMMA was purchased from Aldrich designated by the abbreviation Com-PMMA. The molecular weight of Com-PMMA was determined by Size Exclusion Chromatography and is about $M_w = 90{,}000\ g\ mol^{-1}$ using a PMMA standard calibration curve.

Snowtex silica nanoparticles, purchased from Nissan, were in isopropanol solution at a concentration of 30% in weight and about 12 nm in diameter.

2.1.2. Preparation of class II hybrid thin films

The synthesis of the triethoxysilane functionalized PMMA as well as the preparation of class II PMMA-SiO_2 hybrid thin films by in situ polymerisation of TEOS in PMMA were described in the part I paper.

Hybrid nanoparticles based solutions were obtained by adding 15% and 25% in weight of *Snowtex* nanoparticles to a solution of a triethoxysilane functionalized PMMA in THF (the concentration of f-PMMA was $1\ g\ L^{-1}$). The sols were vigourously stirred at room temperature (RT) for 30 min before deposition.

2.1.3. Preparation of class I hybrid thin films

Hybrid solutions were obtained by adding 75, 50 and 25% in mol of pre-hydrolyzed TEOS to a solution of a free triethoxysilane functionalized PMMA in THF (the concentration of Com-PMMA was $1\ g\ L^{-1}$). Si/PMMA: 25/75, 50/50, 75/25, noted Com-PMMA*x*, where *x* is the molar ratio of the commercial PMMA. The sols were vigorously stirred at RT for 48 h before deposition.

Before deposition, the substrates were cleaned using a soap solution, followed by rinsing in demineralized water allowing to obtain an hydrophilic surface. The films were spin-coated on standard float glass (Saint-Gobain) and cured at 100 °C for 8 h. All films compositions and characteristics are listed in Table 1.

2.2. Characterizations

^{29}Si MAS NMR data were recorded on a AV300 Brucker spectrometer (59.62 MHz) using 7 mm diameter zircona

Table 1
Thin films mechanical characteristics

Sample	Class – % in weight of SiO_2	Aspect	Thickness (nm)	E (GPa)[a]	H (GPa)[a]
Com-PMMA	I – 0	Transparent	1490	6.90	0.32
Com75	I – 17	Translucent	1160	6.30	0.45
Com50	I – 43	Transparent	2220	8.20	0.56
Com25	I – 76	Opaque	2450	–	–
f-PMMA	II – 0	Transparent	1790	4.10 ± 0.40	0.25 ± 0.03
PMMA75	II – 22	Transparent	1680	7.60 ± 0.80	0.50 ± 0.05
PMMA50	II – 47	Transparent	2030	6.60 ± 0.70	0.54 ± 0.06
PMMA25	II – 72	Transparent	1890	9.50 ± 1.00	0.85 ± 0.09
Hyb85	II – 15	Transparent	1080	6.90 ± 0.70	0.33 ± 0.03
Hyb75	II – 26	Transparent	1080	8.30 ± 0.80	0.40 ± 0.04

[a] Determined by applying the models of Mencik et al. and Bhattacharya et al.

rotors at a spinning frequency of 4 kHz. The spectra were then fitted using the WIN-FIT[24] program in order to characterize the hybrid interface between the polymer and the oxide components.

The molecular weight of the organic polymer was determined by size exclusion chromatography (SEC) in THF at a flow rate of 0.8 mL min^{-1} and using a PMMA standard calibration curve (Waters apparatus); the porosity of the μ-styragel columns was 10^5, 10^4, 10^3, 500 and 100 Å.

Scanning electron microscopy (SEM) with field gun (Leo Gemini DSM 982) allowed us to determine the layer thickness (average value of four different measurements on images observed in the secondary electrons mode). Furthermore, the backscattered electrons mode was used to characterize the phase separation at the sub-micronic scale.

Thermogravimetric analysis (TGA) performed on the xerogels allowed to determine the organic to inorganic ratio and the thermal stability of the hybrid materials; the heating rate was 10 °C min^{-1}. All thermal analysis were performed in oxygen and nitrogen atmospheres.

Nanoindentation experiments were performed at RT using a NanoHardness Tester machine from CSEM (Switzerland). Procedures and analysis developed for PMMA-SiO_2 hybrid coatings were described in the part I paper.

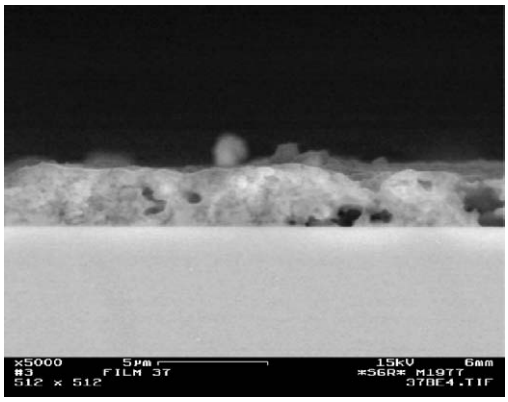

Fig. 1. Observation of the cross-section of an inorganic class I coating (Com25) in the backscattered electrons mode of the SEM.

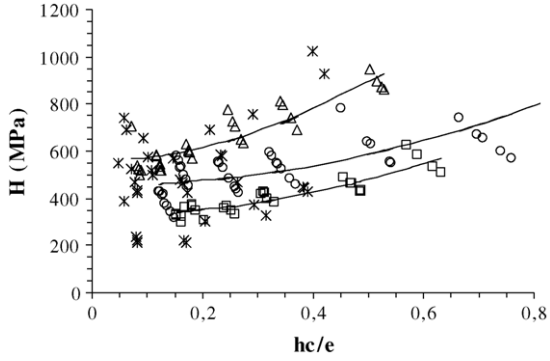

Fig. 2. Evolution of hardness H as a function of the relative indentation depth h_c/e for class I hybrid thin films (□) Com-PMMA, (◯) Com75, (△) Com50, (✱) Com25.

3. Results

3.1. Sol–gel silica based hybrid thin films

The obtained class I, Com-PMMA*x* hybrid thin films were not transparent contrary to the class II hybrid thin films but they are translucent to opaque according to the composition of the layers as reported in Table 1: while Com-PMMA and Com50 are transparent, Com75 is translucent and Com25 is opaque due to a phase separation between polymer and silica which can be observed by SEM (Fig. 1).

The relative amounts of Q_n units in class II hybrids samples are reported in Table 2; the silica network is mainly made of about 50% Q_4, 40% Q_3 and 10% Q_2 species.

The indentation load–displacement curves allow to determine the indentation modulus and hardness as a function of indentation depth to thickness ratio (Fig. 2).[25,26] Indentation modulus and hardness increase with the relative indentation depth because of the substrate contribution to the mechanical responses. However, hardness increases less rapidly than indentation modulus as reported and discussed previously for class II PMMA-SiO_2 coatings. It should be noted that the scatter in the mechanical response prevents us from determining the mechanical properties of the sole thin hybrid coating especially in the case of Com-PMMA25 film. The scatter depends on the organic to inorganic composition and is more pronounced when the content of silica is increased, due to inhomogeneity.

The mechanical properties of similar class II hybrid materials prepared by in situ polymerisation of TEOS in a functionalized PMMA were reported in the companion paper and are summarized in Table 1. Such thin films were transparent and their mechanical behaviours were more reproducible

Table 2
Relative amounts of Q_n units in class II hybrid samples and in *Snowtex* silica nanoparticles

Sample	Q_2		Q_3		Q_4	
	δ (ppm)	Percent	δ (ppm)	Percent	δ (ppm)	Percent
PMMA75	−91.5	14	−100.5	47	−108.8	39
PMMA50	−90.9	12	−100.5	47	−109.3	41
PMMA25	−91.5	10	−100.7	45	−110.0	45
Snowtex	−93.0	2	−101.0	21	−110.0	77

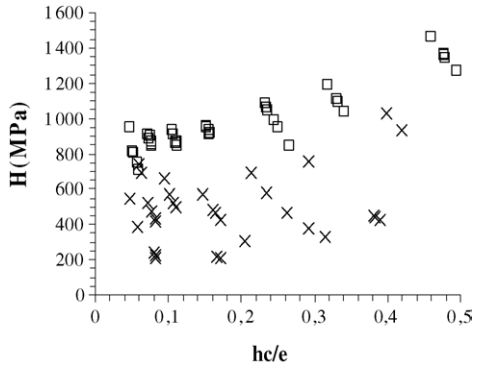

Fig. 3. Evolution of hardness H as a function of the relative indentation depth h_c/e for (□) PMMA25 (class II) and (×) Com25 (class I).

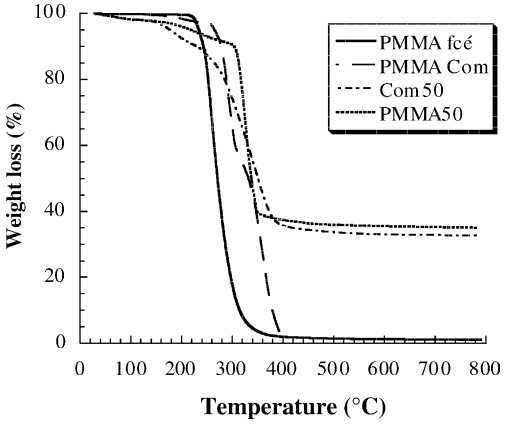

Fig. 4. Thermogravimetric curves performed under oxygen atmosphere of PMMA50 (class II) and Com50 (class I).

(Fig. 3). The mechanical properties of class II hybrid coatings were determined to be more elevated than those measured here for class I films (Table 1).

In the same way, the thermal stability of class II and class I hybrids, determined by thermogravimetric analysis, differs. Thus, the triethoxysilane functionalized PMMA showed lower molecular weight and lower thermal stability than the free triethoxysilane PMMA. On the other hand, the onset of the degradation is observed at a higher temperature for class II materials than for class I (PMMA50 and Com50 for example) ones despite the reverse trend obtained for neat polymers (Fig. 4). In fact, for a given organic/inorganic composition, class II materials showed a better thermal stability than class I materials.

3.2. Silica nanoparticles based hybrid thin films

Class II hybrid thin films prepared by mixing silica preformed nanoparticles and a functionalized PMMA were all transparent and homogeneous. No phase separation was observed by SEM-FG in good agreement with the optical aspect of the films.

The relative amounts of Q_n units in *Snowtex* silica are reported in Table 2; the nanoparticles are made of 80% Q_4 and 20% Q_3 species.

Fig. 5 plots the hardness and reduced modulus as a function of the h_c/e ratio. The mechanical properties showed an increase with the increase of silica in the layer even though only a slight reinforcement of the PMMA by silica is observed in the range of compositions investigated here (Fig. 5). The behaviour of the mechanical response was observed to be similar to that of PMMA-SiO_2 prepared by in situ polymerisation of TEOS in PMMA and both indentation modulus and hardness could be determined for the sole thin films (Table 1). Interestingly, nanoparticles based hybrid thin films showed lower hardness than sol–gel silica based hybrids while the reduced modulus was found to be very close for both films (Fig. 6).

4. Discussion

4.1. Strength of the intercations between organic and inorganic components: contribution of the covalent bonds

A good homogeneity of hybrid materials can be achieved if weak interactions developed between both components, are sufficient to create a good interpenetration of the two networks at the molecular scale. Hydroxyl groups Si-OH, generated by sol–gel chemistry, exhibit Brønsted acidity (when the hydrolysis and condensation of molecular precursors is

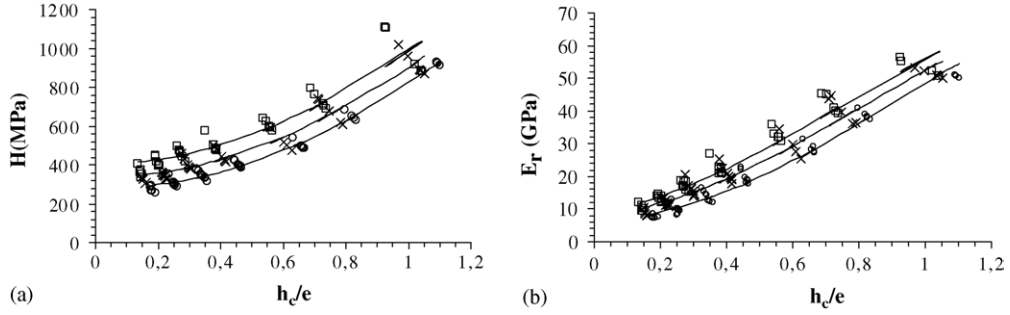

Fig. 5. Evolution of (a) the indentation modulus, (b) the hardness as a function of the relative indentation depth h_c/e of class II nanoparticles based hybrid thin films of (◯) f-PMMA, (×) Hyb85 and (□) Hyb75.

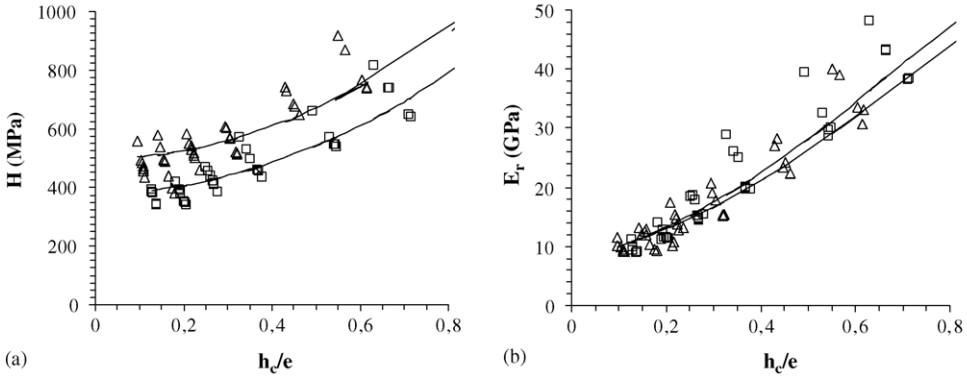

Fig. 6. Evolution of (a) the indentation modulus and (b) the hardness as a function of the relative indentation depth h_c/e of (□) Hyb75 and (△) PMMA75.

acidic catalyzed) whereas carbonyl groups along the polymer macromolecules are well-known to be strong acceptors of acidic hydrogen and to form hydrogen bonds.[1,19]

The size of the phase separation between organic and inorganic components can be varied from the submicronic to the nanometer scale in several ways. In order to minimize the phase segregation, one of them consists of the formation of covalent bonds between the polymer and the silica phases by an appropriate functionalization of the organic component, leading to class II materials.[23,13] Class I thin films are observed to be opaque or translucent because no covalent interactions exist to hinder phase separation; moreover, the hydrogen bonding between PMMA and sol–gel silica is in this case too weak to prevent phase separation. Consequently, it is advantageous to use a coupling agent in the preparation of hybrid organic–inorganic materials because of the formation of covalent interactions between both components which prevents the phase separation between the organic polymer and the silica network (avoiding the formation of silica particles).

Indentation modulus and hardness increase with the relative indentation depth because of the substrate contribution to mechanical properties as discussed in more details in the companion paper (part I). The scatter of the mechanical response occurred only for some of the class I hybrids and is to be correlated to the degree of phase separation within these specimens. When a phase separation occurs between the polymer and the silica (Com25 coating), the thin film is opaque and the mechanical properties cannot be determined due to the scattered nanoindentation responses. On the other hand, the mechanical properties can be determined for all transparent coatings (in which covalent bonds are established between organic and inorganic components). Consequently, instrumented nanoindentation is sensitive to the morphology of the sample, which is governed by the nature of the interface. The distance between indents was typically 30 μm so that we conclude that mechanical inhomogeneity is at a scale less than 30 μm. Moreover, covalent bonds established between the organic and inorganic components led to an increase in the degradation temperature of the PMMA; these observations are in good correlation with the measured values of indentation modulus and hardness which were found to be higher for class II than for class I materials.

4.2. Size of the hybrid interface between PMMA and silica

When silica is introduced as particles, the influence of the size of the interface can be investigated comparing their behaviour to that of PMMA-TEOS where molecular-sized silica is formed as discussed in more details below. Larger hybrid interfaces are developed when sol–gel silica is generated by the in situ polymerisation of TEOS in PMMA than when nanoparticles are used.[27,28] Indeed, the relative proportions of the Q_n species allowed us to conclude that *Snowtex* silica is more condensed than the sol–gel silica. The abundance of Q_3 species in sol–gel silica led to more hydrogen bonding between the silanols groups and the carbonyle of PMMA and both organic and inorganic components are mixed at a molecular level; all interactions (covalent and hydrogen bonds) promote a decrease in the polymer mobility (part I) and an increase in the hardness as the size of the interface is increased. In the same way, thermal stability of hybrid PMMA-SiO_2 was improved by generating in situ sol–gel silica in PMMA than by using silica nanoparticles.

5. Conclusion

The versatile experimental conditions of the sol–gel processes allow to elaborate thin films of hybrid materials which exhibit different interfaces between the polymer and the silica network. Using indentation to test mechanical properties, a correlation between structure and mechanical response could be revealed. Thus, class I films showed scattered mechanical responses in good correlation with the phase separation detected in cross-sectional SEM measurements. Moreover, class II materials were found to have better mechanical properties than class I. The extent of the hybrid interface could be adjusted by the use of preformed silica nanoparticles. In situ condensation of TEOS in the organic media leads to a more

extended interface with H bondings and covalent bondings. We showed that the mechanical response is governed by the size of the hybrid interface since the mechanical properties of materials based on sol–gel silica are more elevated than those obtained from materials formed from silica nanoparticles which exhibit a more defined interface.

Acknowledgements

The authors want to thank Saint-Gobain Recherche for financial support and especially Laurent Delattre, Arnaud Huignard and Didier Lefèvre for helpful discussions and Laure Castel for SEM analyses. Jocelyne Maquet (LCMC) is acknowledged for NMR experiments.

References

1. Brinker, C.J. and Scherrer, G.W., *Sol–Gel Science—the Physics and Chemistry of Sol–Gel Processing*. San Diego 1990.
2. Livage, J., Henry, M. and Sanchez, C., *Prog. Solid State Chem.*, 1988, **18**(4), 259–341.
3. Schmidt, H., Kaiser, A., Patzelt, H. and Scholze, H., *J. Phys.*, 1982, **12**, C9–C275.
4. Wilkes, G. L., Orler, B. and Huang, H. H., *Polym. Prep.*, 1985, **26**, 300–301.
5. Wilkes, G. L., *Mater. Res. Soc. Symp. Proc.*, 1990, **171**, 15–29.
6. Sur, G. S. and Mark, J. E., *Eur. Polym. J.*, 1985, **21**, 1051–1052.
7. Morikawa, A., Iyoku, Y., Kakimoto, M. and Imai, Y., *J. Mater. Chem.*, 1992, **2**, 679–689.
8. Chujo, Y. and Saegusa, T., *Adv. Polym. Sci.*, 1992, **100**, 11.
9. Novak, B. M., *Adv. Mater.*, 1993, **5**(6), 422–433.
10. Loy, D. A. and Shea, K. J., *Chem. Rev.*, 1995, **95**, 1431–1442.
11. Corriu, R. J. P. and Leclercq, D., *Angew. Chem. Int. Ed.*, 1996, **35**, 1421–1436.
12. Schubert, U., Huesing, N. and Lorenz, A., *Chem. Mater.*, 1995, **7**(11), 2010–2027.
13. Sanchez, C. and Ribot, F., *New J. Chem.*, 1994, **18**(10), 1007–1047.
14. Ribot, F. and Sanchez, C., *Comments Inorg. Chem.*, 1999, **20**(4–6), 327–371.
15. Sanchez, C., Soler-Illia, G. J. d. A. A., Ribot, F., Lalot, T., Mayer, C. R. and Cabuil, V., *Chem. Mater.*, 2001, **13**(10), 3061–3083.
16. Schubert, U., *Chem. Mater.*, 2001, **13**(10), 3487–3494.
17. Sanchez, C., Lebeau, B., Chaput, F. and Boilot, J.-P., *Adv. Mater.*, 2003, **15**(23), 1969–1994.
18. Landry, C. J. T. and Coltrain, B. K., *Polymer*, 1992, **33**(7), 1486–1495.
19. Landry, C. J. T., Bradley, K. C., Wesson, J. A. and Lippert, J. L., *Polymer*, 1992, **33**(7), 1496–1506.
20. Abramoff, A. and Klein, L. C., *SPIE*, 1990, **1328**, 241–248.
21. Pope, E. J. A., Asami, M. and Mackenzie, J. D., *J. Mater. Res.*, 1989, **4**(4), 1018–1026.
22. Bourgeat-Lami, E., *J. Nanosci. Nanotech.*, 2002, **2**(1), 1–24.
23. Coltrain, B. K., Landry, C. J. T., O'Reilly, J. M., Chamberlain, A. M., Rakes, G. A., Sedita, J. S. *et al.*, *Chem. Mater.*, 1993, **5**(10), 1445–1455.
24. Massiot, D., Fayon, F., Capron, M., King, I., Le Calve, S., Alonso, B. *et al.*, *Magn. Reson. Chem.*, 2002, **40**, 70–76.
25. Bhattacharya, A. K. and Nix, W., *Int. J. Solids Struct.*, 1988, **24**, 1287–1298.
26. Mencik, J., Munz, D., Quandt, E., Weppelmann, E. R. and Swain, M. V., *J. Mater. Res.*, 1997, **12**(9), 2475–2484.
27. Guermeur, C., Lambard, J., Gérard, J. F. and Sanchez, C., *J. Mater. Chem.*, 1999, **9**(3), 769–778.
28. Sanchez, C., Ribot, F., Rozes, L. and Alonso, B., *Mol. Cryst. Liq. Cryst.*, 2000, **354**, 143–158.